

Chapter 4 大氣長波輻射

4-1 溫室效應(greenhouse effect)

$$S \cdot \pi a_e^2 (1 - \bar{r}) = \sigma T_e^4 \cdot 4\pi a_e^2 \quad (4.1)$$

S * sectional area * absorb = I of earth*surface

where S : 太陽常數

a_e : 地球半徑

\bar{r} : 全球平均反照率

T_e : 地球的平衡溫度

$$\rightarrow T_e = [S(1 - \bar{r})/4\sigma]^{1/4} \quad (4.2)$$

$$\approx 255\text{K}$$

但是地球的平均表面溫度約 288°K，遠高於從(4.2)所得到平衡溫度，其主要原因為溫室效應

溫室效應主要是因為大氣吸收了某波段的地球長波輻射，所以能量被保留在大氣中。

Atmospheric blind channel (absorbed)
Atmospheric window channel (pass)

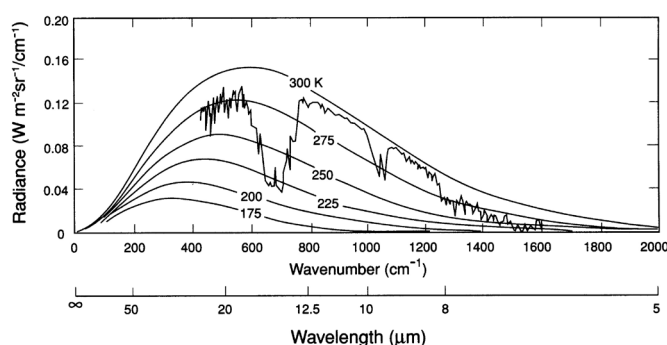


Fig 4.1: Theoretical Planck radiance curves for a number of the earth's atmospheric temperatures as a function of wavenumber and wavelength. Also shown is a thermal infrared emission spectrum observed from the Nimbus 4 satellite based on an infrared interferometer spectrometer. [Liou02, Figure4.1]

從圖 4.1，大氣長波輻射相似於 290°K 的黑體輻射。

CO_2 : $15\ \mu\text{m}$, $600\sim 800\text{cm}^{-1}$, 且在長波輻射最強的地方。

H_2O : $6.3\ \mu\text{m}$, $1200\sim 2000\ \text{cm}^{-1}$; $< 500\ \text{cm}^{-1}$ for rotational band.

O_3 : $9.6\ \mu\text{m}$.

★ → 以 $5\ \mu\text{m}$ 為界線，分為長波和短波輻射

4-2 大氣的吸收與放射

4-2-1 紅外線的吸收

<a> 水氣

水氣主要的吸收光譜有 $2.7\ \mu\text{m}$ (rotational band) 、 $6.3\ \mu\text{m}$ (vibrational –rotational band) 和 $10\ \mu\text{m}$ (waters vapor continuum) 。 $0-1000\text{cm}^{-1}$ 的水氣吸收光譜對於對流層的冷卻相當重要，其為 rotational band 。 1000000 lines

 二氧化碳

最重要的吸收光譜為 $15\ \mu\text{m}$ ，其中包含了許多條吸收光譜的組合。

<c> 臭氧

為主要的吸收光譜為 $9.6\ \mu\text{m}$ (vibrational) ，其為大氣窗 ($800-1200\text{cm}^{-1}$) 中主要的吸收光譜。

其他溫室氣體包括了 CH_4 , N_2O 和 CH_3CL 等氟氯碳化物。

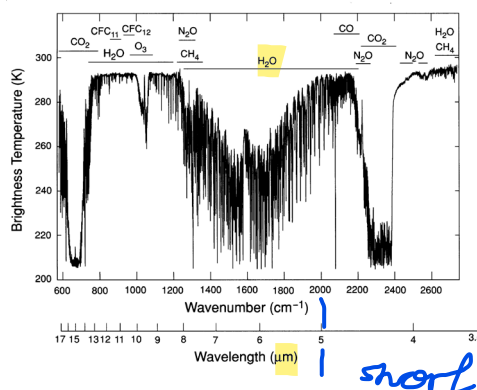


Fig 4.2: Observed infrared spectrum displaying all the absorption gases and their spectral location. This spectrum was obtained from the scanning high-resolution interferometer sounder (S-HIS), which measured the emitted thermal radiation between 3.3 and $18\ \mu\text{m}$, onboard the NASA ER-2 aircraft over the Gulf of Mexico southeast of Louisiana on April 1, 2001 (courtesy of Allen Huang and Dave Tobin of the University of Wisconsin). [Liou02, Figure4.3]

4-2-2 基本紅外線傳遞方程

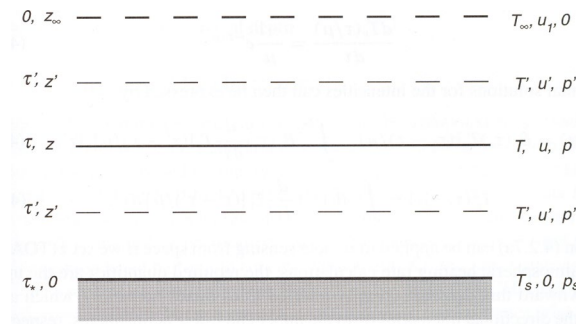


Fig 4.3: Coordinate systems in τ, z, u, T , and p for IR radiative transfer in plane-parallel atmospheres. U is the path length for absorbing gases defined from the surface upward. The total path length is denoted by u_1 . T_∞ and z_∞ are temperature and height, respectively, at TOA. The surface temperature $T_s = T(\tau_*)$. The surface pressure is denoted by p_s . [Liou02, Figure4.4]

法線光程

$$\tau = \int_z^{z_\infty} k_v(z') \rho_a(z') dz' = \int_0^p k_v(p') q(p') \frac{dp'}{g} \quad (4.3)$$

with $\frac{dp}{dz} = -\rho g$

where $q = \rho_a / \rho$, ρ 為空氣密度， g 為重力加速度

所以 q 為氣體混合比， ρ_a 為吸收氣體密度

e.g., if ρ_a is water vapor

→ q is mixing ratio of water vapor

參考(2.34)，則傳遞方程可寫成

$$\mu \frac{dI_v(\tau, \mu)}{d\tau_v} = I_v(\tau, \mu) - B_v(\tau)$$

根據平行大氣假設(section 2-3-4)，且大氣的總光程為 τ_*

假設地表為黑體輻射，i.e. $I_v(\tau_*, \mu) = B_v(\tau_*)$

假設大氣層頂向下的長波輻射 $B_v(top) \cong 0$



$$I_v^\uparrow(\tau, \mu) = B_v(\tau_*) e^{-(\tau_* - \tau)/\mu} + \int_\tau^{\tau_*} B_v(\tau') e^{-(\tau' - \tau)/\mu} \frac{d\tau'}{\mu} \quad (4.4a)$$

$$I_v^\downarrow(\tau, -\mu) = \int_0^\tau B_v(\tau') e^{-(\tau - \tau')/\mu} \frac{d\tau'}{\mu} \quad (4.4b)$$

Defining 單色透射率

$$\frac{dI_v}{d\tau/\mu} = I_v$$

$$\rightarrow \frac{dI_v}{I_v} = \frac{d\tau}{\mu}$$

$$\rightarrow \int_{I_0}^{I_v} \frac{dI_v}{I_v} = \int_{\tau}^0 \frac{d\tau}{\mu}$$

$$\begin{aligned} \frac{I_v}{I_0} &= e^{-\tau/\mu} \\ &= T_v(\tau/\mu) \end{aligned}$$

$$\boxed{T_v(\tau/\mu) = e^{-\tau/\mu}} \quad \text{simplify transmit} \quad (4.5a)$$

$$\rightarrow \frac{dT_v(\tau/\mu)}{d\tau} = \frac{-1}{\mu} e^{-\tau/\mu} \quad (4.5b)$$

(4.4) →

$$I_v^{\uparrow}(\tau, \mu) = B_v(\tau_*) \underline{T_v[(\tau_* - \tau)/\mu]} - \int_{\tau}^{\tau_*} B_v(\tau') \frac{d}{d\tau'} \underline{T_v[(\tau' - \tau)/\mu]} d\tau' \quad (4.6a)$$

$$I_v^{\downarrow}(\tau, -\mu) = \int_0^{\tau} B_v(\tau') \frac{d}{d\tau'} T_v[(\tau - \tau')/\mu] d\tau' \quad (4.6b)$$

對於輻射通量密度(此後簡化為通量(flux)) (參考(2.9))

Following section 2-1-3,

$$F_v^{\uparrow\downarrow} = \int_0^{4\pi} I_v^{\uparrow\downarrow} \cos \theta d\Omega$$

$$d\Omega = \sin \theta d\theta d\varphi$$

$$\rightarrow F_v^{\uparrow\downarrow}(\tau) = \int_0^{2\pi} \int_0^{\pi/2} I_v^{\uparrow\downarrow}(\tau, \pm\mu) \cos \theta \sin \theta d\theta d\varphi$$

$$= \int_0^1 I_v^{\uparrow\downarrow}(\tau, \pm\mu) \mu d\mu \int_0^{2\pi} d\varphi$$

$$\rightarrow F_v^{\uparrow\downarrow}(\tau) = 2\pi \int_0^1 I_v^{\uparrow\downarrow}(\tau, \pm\mu) \mu d\mu \quad (4.7)$$

Defining 通量透射率(diffuse transmittance)

$$T_v^f(\tau) = 2 \int_0^1 T_v(\tau/\mu) \mu d\mu \quad (4.8)$$

(4.7)→

$$F_v^\uparrow(\tau) = \pi B_v(\tau_*) T_v^f[(\tau_* - \tau)] - \int_\tau^{\tau_*} \pi B_v(\tau') \frac{d}{d\tau'} T_v^f[(\tau' - \tau)] d\tau' \quad (4.9a)$$

$$F_v^\downarrow(\tau) = \int_0^\tau \pi B_v(\tau') \frac{d}{d\tau'} T_v^f[(\tau - \tau')] d\tau' \quad (4.9b)$$

物理意義：

<1>向上通量的兩個來源：**地表的長波輻射經過大氣的削弱過程**和**大氣的長波輻射經由黑體輻射×比例函數**($dT_v^f/d\tau$)。

<2>向下通量的主要來源則為大氣的長波輻射。

對於所有的波數而言

$$F^{\uparrow\downarrow}(z) = \int_0^\infty F_v^{\uparrow\downarrow}(z) dv \quad (4.10)$$

為了簡化輻射計算

$$T_v^f(\tau) \cong T_{\bar{v}}(\tau/\bar{\mu}) \quad (4.11)$$

where $1/\bar{\mu}$ 在 1.66 與 2 之間

$$\rightarrow \bar{\theta} \approx 53^\circ \sim 60^\circ$$

將(4.5a)代入(4.11)即可得到 $T_v^f(\tau)$

物理意義：對於方向輻射的總和，可由($\bar{\mu}$ 方向的輻射×常數)估計

討論：<1>**向上和向下**輻射的總量可用 $\pm \bar{\mu}$ 方向的輻射強度估計

→ **二流近似法** (two-stream approximation) [simplify Tv calculate](#)

<2>比較(2.11)，對於無方向性(isotropic)輻射而言，

$$F_v = \pi I_v = \pi B_v T_{\bar{v}}^f$$

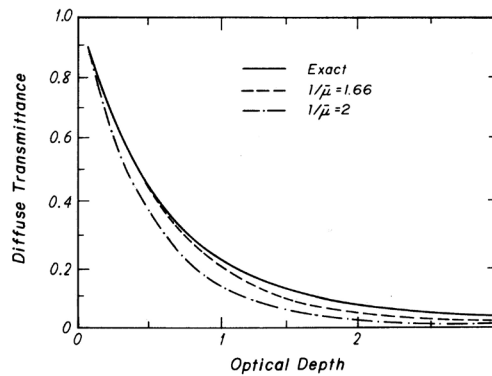


Fig 4.4: The diffuse transmittance as a function of the optical depth for three cases. [Liou92, Figure2.8]

4-2-3 單線積分法(line-by-line integration)

令 $du = \rho ds$ ，其中 u 為吸收體含量

$$\tau(\square \square) = \sum_{j=1}^N \tau_j = \int_u \sum_{j=1}^N k_{v,j}(u) du \quad (4.12)$$

$k_{v,j}$ (吸收係數) 是 N 條吸收光譜的總和 (例如振動、旋轉、和能階跳躍)，而 $k_{v,j}$ 可寫成光譜強度 (S_j) 和型狀 ($f_{v,j}$) 的函數

$$k_{v,j}(P, T) = S_j(T) f_{v,j}(P, T) \quad (4.13)$$

➔ 對於波段 Δv 而言，平均通量透射率

$$\begin{aligned} T_{\bar{v}}(u) &= \int_{\Delta v} \exp\left(-\int_u k_v(u) du\right) \frac{dv}{\Delta v} \\ &= \int_{\Delta v} \exp\left(-\int_u \sum_j k_{v,j}(u) du\right) \frac{dv}{\Delta v} \\ &= \sum_i \exp\left(-\int_u \sum_j k_{i,j}(u) du\right) \frac{\Delta v_i}{\Delta v} \\ &= \sum_i \exp\left(-\sum_n \sum_j k_{i,j}(P_n, T_n) \Delta u_n\right) \frac{\Delta v_i}{\Delta v} \quad \text{1e6 calculate times} \quad (4.14) \end{aligned}$$

所以計算 $T_{\bar{v}}(u)$ 是個非常耗時的過程，包含了 i 個波段 (Δv)， j 條吸收光譜和 n 層非均勻大氣。同時吸收係數又與吸收光譜的強度有關，且吸收光譜強度是溫度和氣壓的函數。為了簡化其計算過程，則發展了下列即將要討論的方法。

4-3 修正的 k-分佈法(corrected k-distribution method)

k-分佈法的基本概念是將通量透射率從波數的函數轉成吸收函數(k)的函數。在平均的大氣中，

$$T_{\bar{\nu}}(u) = \int_{\Delta \nu} e^{-k_{\nu} u} \frac{d\nu}{\Delta \nu} = \int_0^{\infty} e^{-ku} f(k) dk \quad (4.15)$$

where $f(k)$ 是正規化(normalized)的機率分佈函數

令 k_{\min} (最小值的 k) $\rightarrow 0$ 和 $k_{\max} \rightarrow \infty$ (最大值的 k)

$$\int_0^{\infty} f(k) dk = 1 \quad (4.16)$$

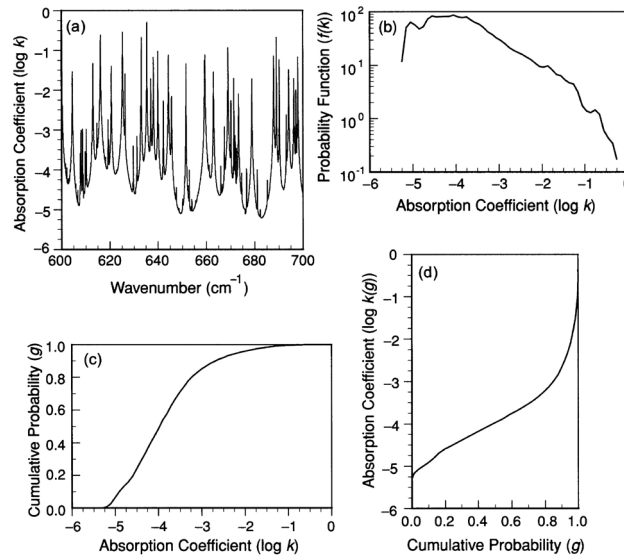


Fig 4.5: (a) Absorption coefficient k_{ν} in units of $(\text{cm atm})^{-1}$ as a function of wavenumber with a resolution of 0.01 cm^{-1} in the H_2O rotational band with $p=600 \text{ mb}$ and $T=260 \text{ K}$. (b) The probability function $f(k)$ of the absorption coefficient. (c) The cumulative probability function for $f(k)$ shown in (b), k plotted as a function of k . (d) Same as (c), except that values of the absorption coefficient are expressed as a function of g . [Liou02, Figure4.5]

4-4 帶模式(Band model)

Defining 波段平均吸收率

$$A_v(u) = 1 - T_v = \frac{1}{\Delta v} \int_{\Delta v} 1 - e^{-k_v u} dv \quad (4.17)$$

而 $A_v(u)\Delta v$ 相等於寬度($W(u)$)

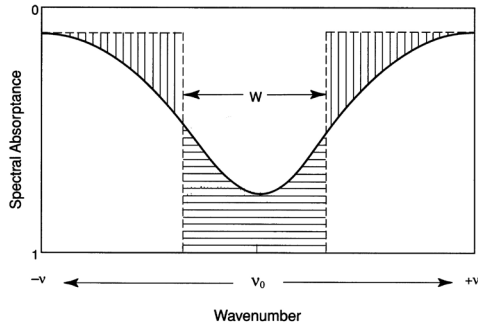


Fig 4.6: The definition of equivalent width, $W = A_v \Delta v$, where A_v represents the spectral absorbance for a spectral interval Δv . It is the width of an infinitely strong line of rectangular shape that is the same as the absorption of a single line. [Liou02, Figure4.9]

4-5 寬帶(broad band)的觀念

主要的原理是定義一個寬帶通量放射率—即對所有的波長做積分，以求得一個平均的通量放射率。即直接用 Stefan-Boltzmann Law 取代 Planck function，其中有效而最常用的假設是等溫寬帶通量放射率。

4-6 長波輻射傳遞方程在有雲的大氣

4-6-1 基本方程

當有雲時，我們必須考慮長波散射過程。對於散射所產生的能量來源 J_v 而言，傳遞方程可寫成

$$\begin{aligned} \mu \frac{dI_v}{dz} &= -\beta_e I_v + \beta_a B_v + \beta_s J_v \\ &= -(\beta_a + \beta_s) I_v + \beta_a B_v + \beta_s J_v \\ \rightarrow \mu \frac{dI_v}{dz} &= -\beta_a (I_v - B_v) - \beta_s (I_v - J_v) \\ &= -\beta_e (I_v - S_v) \end{aligned} \quad (4.18)$$

$$\text{where } S_v = (\beta_a B_v + \beta_s J_v) / \beta_e \quad (4.19a)$$

假設 $\tilde{\omega} = \beta_s / \beta_e$ 為單次散射反照率 (single-scattering albedo)

(4.19a)→

$$S_v = (1 - \tilde{\omega}_v) B_v + \tilde{\omega}_v J_v \quad (4.19b)$$

對於長波輻射而言，我們只需考慮天頂角方向的分量(why?)，所以

$$J_v = \frac{1}{2} \int_{-1}^1 P(\mu, \mu') I_v(\tau, \mu') d\mu' \quad (4.20)$$

其中，相位函數

$$P(\mu, \mu') = \frac{1}{2\pi} \int_0^{2\pi} P(\cos \Theta) d\phi' \quad (4.21)$$

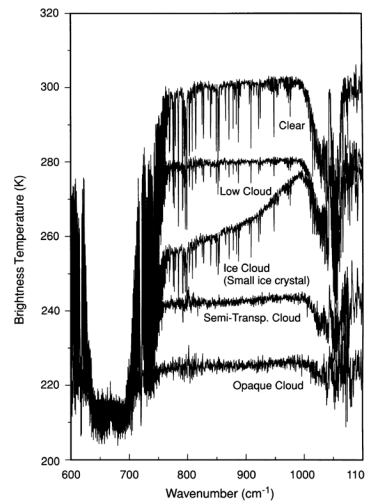


Fig 4.7: Spectra of brightness temperature observed from a high spectral resolution infrared spectrometer from the high-flying ER-2 aircraft over a domain, 37.1°–37.4° N, 95.0°–95.3° W, on April 21, 1996, indicating wavelength-dependent window brightness temperature changes according to various cloud types. The type of cloud indicated for each spectrum is identified from the Cloud Lidar System aboard the ER-2 (data taken from Smith *et al.*, 1998). [Liou02, Figure4.12]

含水的雲對長波而言為黑體，但含冰的雲則不是黑體。

Fig 4.7 所指的波長範圍為 9.1 到 17 μm 且在 20km 高空所測量的。

<i>9.6 μm (1040 cm^{-1}) O_3 absorption, 15 μm (667 cm^{-1}) CO_2 absorption 和 10~12 μm (1000~830 cm^{-1}) water vapor scattered lines.

<ii>除 small ice crystal，其餘均為黑體→吸收強度不隨波長改變且其強度和雲頂溫度有關

<iii>ice clouds with small ice crystal(5~20 μm)的強度和波長有關→長波在雲中的散射

4-6-2 雲底和地表所交換的長波輻射

在夜晚，雲是個決定地表溫度的重要因素。

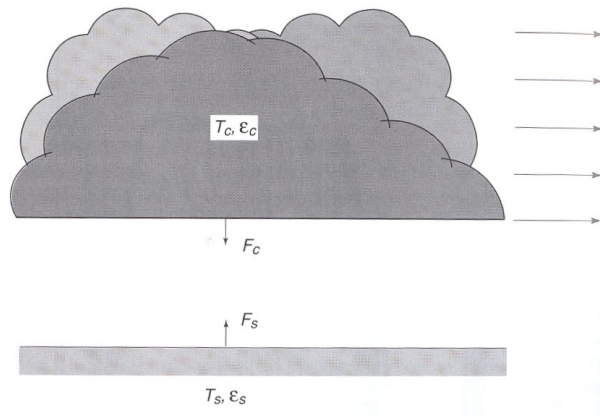


Fig4.8 A simple configuration of a cloud moving over a surface. The surface temperature is modified by the presence of the cloud. [Liou02, Figure4.13].

根據 Fig4.8,

$$F_s^{\uparrow} = \varepsilon_s \sigma T_s^4 + (1 - \varepsilon_s) F_c^{\downarrow}$$

$$F_c^{\downarrow} = \varepsilon_c \sigma T_c^4 + (1 - \varepsilon_c) F_s^{\uparrow}$$

$$\rightarrow F_s^{\uparrow} = [(1 - \varepsilon_s) \varepsilon_c \sigma T_c^4 + \varepsilon_s \sigma T_s^4] / [1 - (1 - \varepsilon_s)(1 - \varepsilon_c)]$$

$$F_c^{\downarrow} = [(1 - \varepsilon_c) \varepsilon_s \sigma T_s^4 + \varepsilon_c \sigma T_c^4] / [1 - (1 - \varepsilon_c)(1 - \varepsilon_s)]$$

假設雲與地表間水汽的作用很小

$$\rightarrow \Delta F_n = F_s^{\uparrow} - F_c^{\downarrow} = \frac{\varepsilon_s \varepsilon_c}{1 - (1 - \varepsilon_s)(1 - \varepsilon_c)} \sigma (T_s^4 - T_c^4)$$

如果雲和地表均為黑體，則雲輻射力

$$\rightarrow \Delta F = \Delta F_n - \Delta F_{clear}$$

$$= \sigma (T_s^4 - T_c^4) - \sigma T_s^4$$

$$= -\sigma T_c^4$$

則地表因雲長波輻射所造成的溫度變化為

$$\Delta T = \Delta t \left(-\frac{1}{\rho c_p} \frac{\Delta F}{\Delta z} \right)$$

4-6-3 二流與四流的估計(two/four-stream approximation)

在(4.11)，說明總通量透射率可用 \bar{u} 方向的透射率來表示。但如果對於複雜的散射(即相位函數非常不平滑)，則需要用更多方向的透射率組合來估計散射，所以有所謂的二流與四流估計法。

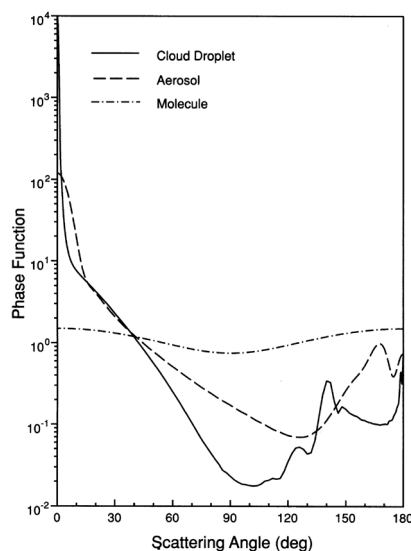


Fig 4.9: Normalized phase functions for cloud droplet ($\sim 10 \mu m$), aerosols ($\sim 1 \mu m$), and molecules ($\sim 10^{-4} \mu m$) illuminated by a visible wavelength of $0.5 \mu m$, computed from the Lorenz-Mie theory. [Liou02, Figure3.13]

e.g. 二流：使用 $\mu = \pm 1/\sqrt{3}$ 的方向來估計 $\rightarrow \theta \approx \pm 55^\circ$

四流：使用 $\mu = \pm 0.2113248$ $\rightarrow \theta \approx \pm 77.8^\circ$ 、

± 0.7886752 $\rightarrow \theta \approx \pm 37.9^\circ$ 四個方向來估計

4-7 大氣長波冷卻率

冷卻率可用下列方程式來表示：

$$\left(\frac{\partial T}{\partial t} \right)_{IR} = - \frac{1}{\rho C_p} \frac{dF(z)}{dz} \quad (4.22)$$

where $F(z) = F^\uparrow(z) - F^\downarrow(z)$ (4.23)

為淨輻射通量

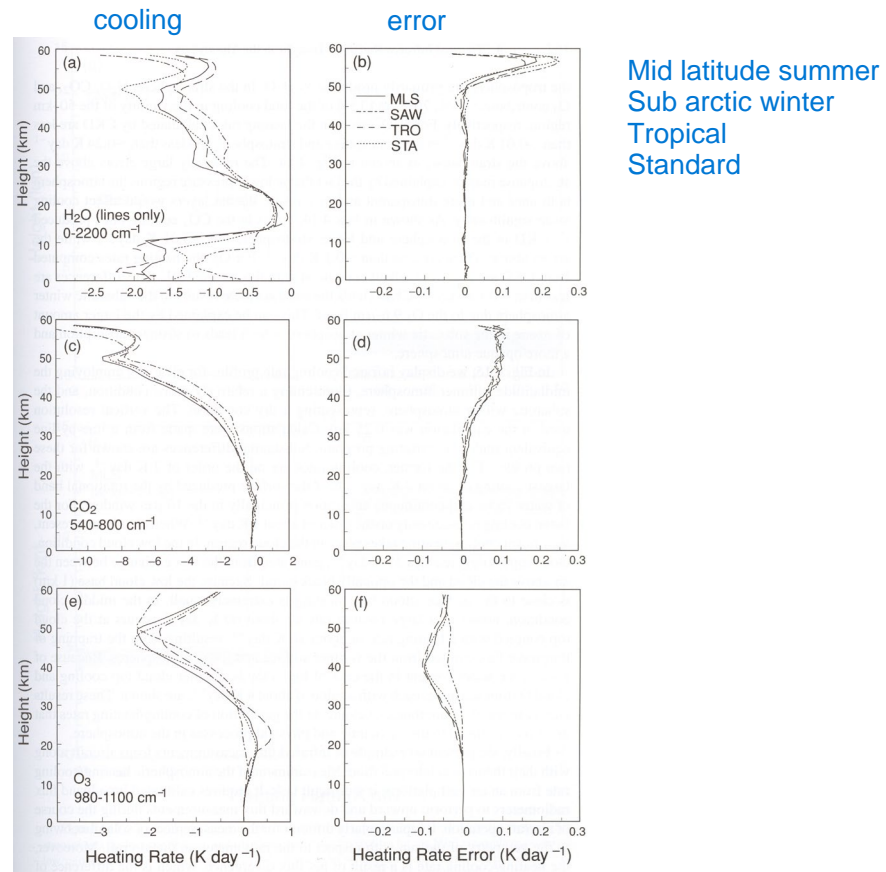


Fig 4.10: Heating rate profiles computed from LBL and the error profiles produced by CKD for the H₂O (a and b), CO₂ (c and d), and O₃ (e and f) bands in the infrared spectrum for the midlatitude summer (MLS), subarctic winter (SAW), tropical (TRO), and U.S. Standard (STA) atmospheres (data taken from Fu and Liou, 1992). [Liou02, Figure4.14]

➔ <i>H₂O cooling is at troposphere and middle atmosphere; at 50km, due to

temperature inversion; at lower atmosphere, $\frac{\partial T}{\partial t} \approx -1 \sim 2^\circ \text{K day}^{-1}$.

<ii> CO₂ cooling is at middle atmosphere where temperature profile is very important.

<iii> O₃ has maximum influence at 20~25km.

<iv> In the troposphere ,cooling is mainly due to H₂O .In the stratosphere, H₂O, CO₂, and O₃ contribute ~15%, 70%, and 15% of the total cooling at 50km.

<v> Larger errors are due to thin air.

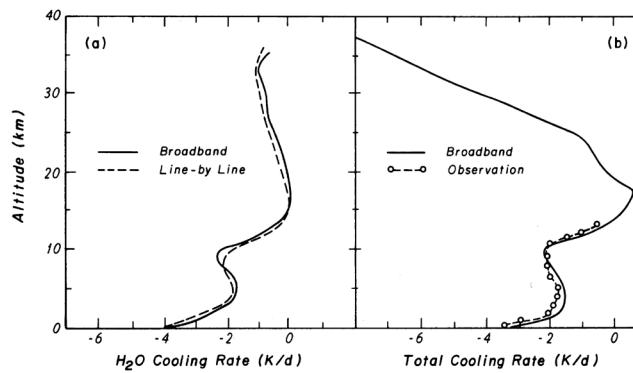


Fig 4.11: (a) Comparison of cooling-rate profiles for water vapor computed from broadband emissivity and line-by-line methods. A tropical atmospheric profile is used in these calculations. (b) Comparison of total cooling-rate profiles for a clear tropical atmosphere computed from the broadband emissivity method with observations in the tropics reported by Cox (1969). [Liou92, Figure2.17]

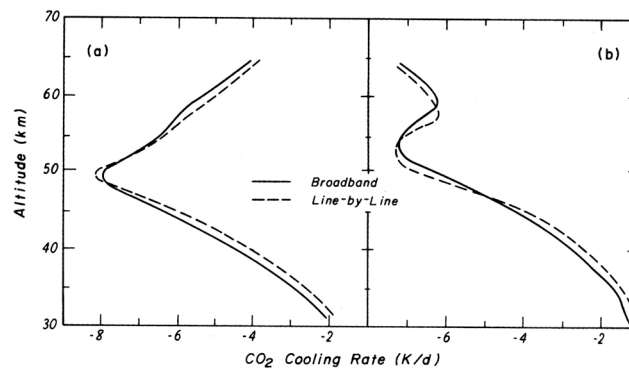


Fig 4.12: comparison of the infrared cooling rates due to the $15\ \mu\text{m}$ CO_2 band computed from the broadband parameterization scheme (Ou and Liou, 1983) with those from the line-by-line method of Fels and Schwazkopf (1981). (a) Standard temperature profile; and (b) polar temperature profile [Liou92, Figure2.18]

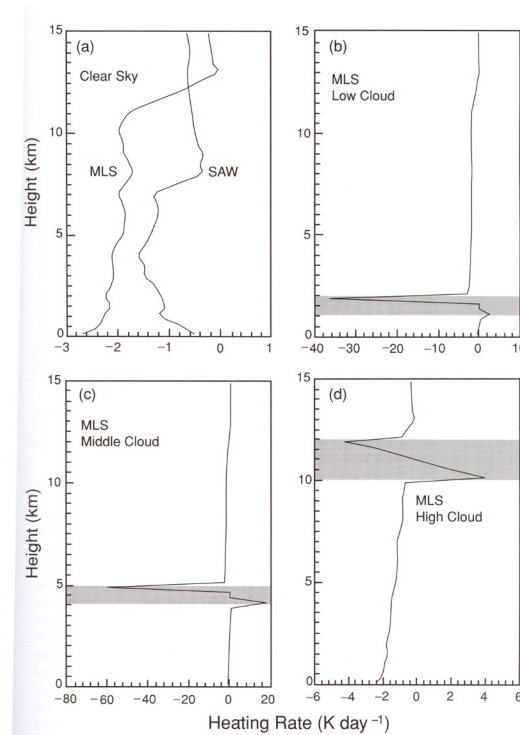


Fig 4.13: (a) Total cooling rates for the midlatitude summer (MLS) and subarctic winter (SAW) atmospheres in clear sky. (b), (c), and (d) display cooling rate profiles for the MLS atmosphere containing low, middle, and high clouds, respectively. The liquid (ice) water content and mean effective radius (size) for these clouds used in the calculations are $(0.22 \text{ g m}^{-3} \text{ and } 5.89 \mu\text{m})$, $(0.28 \text{ g m}^{-3} \text{ and } 6.2 \mu\text{m})$, and $(0.0048 \text{ g m}^{-3} \text{ and } 41.5 \mu\text{m})$, respectively. The locations of these clouds are shaded (data taken from Fu *et al.*, 1997). [Liou02, Figure4.15]

Fig4.13a → In mid-latitude summer, more water vapor → $\frac{\partial T}{\partial t} \approx -2 \sim 3^\circ \text{K day}^{-1}$

In subarctic winter, less water vapor → $\frac{\partial T}{\partial t} \approx -1^\circ \text{K day}^{-1}$

when clouds exist → cloud top cooling and cloud base warming.

magnitudes of cooling and warming depend on cloud water/ice content and cloud top/base temperature.

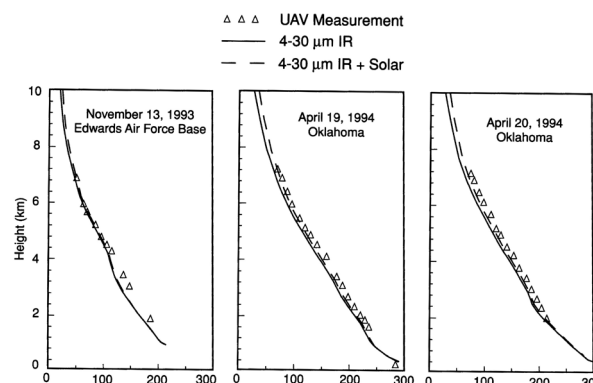


Fig 4.14: Downward infrared fluxes obtained from measurements of unmanned aerospace vehicle (UAV) and from theoretical results for a spectral region covering $4\text{--}30 \mu\text{m}$ with and without including the solar radiation contribution (based on an interim report K.N.Liou submitted to P.Crowley and J.Vitko of the Department of Energy, June 1995). [Liou02, Figure4.16]

→ About 11 W m^{-2} of solar radiation with wavelength greater than $4 \mu\text{m}$.